First Observation of the Hadronic Transition $\Upsilon(4S) \to \eta h_b(1P)$ and New Measurement of the $h_b(1P)$ and $\eta_b(1S)$ Parameters

U. Tamponi,[20,63] R. Mussa,[20] A. Abdesselam,[55] H. Aihara,[60] K. Arinstein,[4] D. M. Asner,[46] H. Atmacan,[35] T. Aushev,[37,21] R. Ayad,[55] I. Badhrees,[55,25] A. M. Bakich,[54] E. Barberio,[34] V. Bhardwaj,[52] B. Bhuyan,[15] J. Biswal,[22] A. Bondar,[4] G. Bonvicini,[65] A. Bozek,[43] M. Bračko,[32,22] T. E. Browder,[12] D. Červenkov,[5] A. Chen,[41] B. G. Cheon,[11] K. Cho,[26] V. Chobanova,[33] S.-K. Choi,[10] Y. Choi,[53] D. Cinabro,[65] M. Danilov,[21,36] Z. Doležal,[5] Z. Drásal,[5] A. Drutskoy,[21,36] S. Eidelman,[4] D. Epifanov,[60] H. Farhat,[65] J. E. Fast,[46] T. Ferber,[7] B. G. Fulsom,[46] V. Gaur,[56] N. Gabyshev,[4] A. Garmash,[4] D. Getzkow,[8] R. Gillard,[65] Y. M. Goh,[11] B. Golob,[30,22] J. Haba,[13,9] K. Hayasaka,[39] H. Hayashii,[40] X. H. He,[47] M. T. Hedges,[12] W.-S. Hou,[42] T. Iijima,[39,38] K. Inami,[38] A. Ishikawa,[59] I. Jaegle,[12] D. Joffe,[24] T. Julius,[34] E. Kato,[59] P. Katrenko,[21] H. Kichimi,[13] C. Kiesling,[33] D. Y. Kim,[51] H. J. Kim,[28] J. H. Kim,[26] K. T. Kim,[27] S. H. Kim,[11] K. Kinoshita,[6] P. Kodyš,[5] S. Korpar,[32,22] P. Križan,[30,22] P. Krokovny,[4] T. Kumita,[62] A. Kuzmin,[4] J. S. Lange,[8] P. Lewis,[12] J. Libby,[16] P. Lukin,[4] D. Matvienko,[4] K. Miyabayashi,[40] H. Miyata,[44] R. Mizuk,[21,36] G. B. Mohanty,[56] A. Moll,[33,57] T. Mori,[38] E. Nakano,[45] M. Nakao,[13,9] T. Nanut,[22] Z. Natkaniec,[43] M. Nayak,[16] N. K. Nisar,[56] S. Nishida,[13,9] S. Ogawa,[58] S. Okuno,[23] S. L. Olsen,[50] W. Ostrowicz,[43] C. Oswald,[3] G. Pakhlova,[37,21] B. Pal,[6] H. Park,[28] T. K. Pedlar,[31] L. Pesántez,[3] R. Pestotnik,[22] M. Petrič,[22] L. E. Piilonen,[64] E. Ribežl,[22] M. Ritter,[33] A. Rostomyan,[7] S. Ryu,[50] Y. Sakai,[13,9] S. Sandilya,[56] L. Santelj,[13] T. Sanuki,[59] Y. Sato,[38] V. Savinov,[48] O. Schneider,[29] G. Schnell,[1,14] C. Schwanda,[18] D. Semmler,[8] K. Senyo,[66] M. E. Sevior,[34] M. Shapkin,[19] V. Shebalin,[4] C. P. Shen,[2] T.-A. Shibata,[61] J.-G. Shiu,[42] B. Shwartz,[4] A. Sibidanov,[54] F. Simon,[33,57] Y.-S. Sohn,[67] A. Sokolov,[19] M. Starič,[22] M. Steder,[7] J. Stypula,[43] K. Tanida,[50] Y. Teramoto,[45] K. Trabelsi,[13,9] M. Uchida,[61] T. Uglov,[21,37] Y. Unno,[11] S. Uno,[13,9] P. Urquijo,[34] C. Van Hulse,[1] P. Vanhoefer,[33] G. Varner,[12] A. Vinokurova,[4] A. Vossen,[17] M. N. Wagner,[8] M.-Z. Wang,[42] X. L. Wang,[64] Y. Watanabe,[23] K. M. Williams,[64] E. Won,[27] J. Yamaoka,[46] S. Yashchenko,[7] Z. P. Zhang,[49] V. Zhilich,[4] V. Zhulanov,[4] and A. Zupanc[22]

(Belle Collaboration)

[1]*University of the Basque Country UPV/EHU, 48080 Bilbao*
[2]*Beihang University, Beijing 100191*
[3]*University of Bonn, 53115 Bonn*
[4]*Budker Institute of Nuclear Physics SB RAS and Novosibirsk State University, Novosibirsk 630090*
[5]*Faculty of Mathematics and Physics, Charles University, 121 16 Prague*
[6]*University of Cincinnati, Cincinnati, Ohio 45221*
[7]*Deutsches Elektronen–Synchrotron, 22607 Hamburg*
[8]*Justus-Liebig-Universität Gießen, 35392 Gießen*
[9]*SOKENDAI (The Graduate University for Advanced Studies), Hayama 240-0193*
[10]*Gyeongsang National University, Chinju 660-701*
[11]*Hanyang University, Seoul 133-791*
[12]*University of Hawaii, Honolulu, Hawaii 96822*
[13]*High Energy Accelerator Research Organization (KEK), Tsukuba 305-0801*
[14]*IKERBASQUE, Basque Foundation for Science, 48013 Bilbao*
[15]*Indian Institute of Technology Guwahati, Assam 781039*
[16]*Indian Institute of Technology Madras, Chennai 600036*
[17]*Indiana University, Bloomington, Indiana 47408*
[18]*Institute of High Energy Physics, Vienna 1050*
[19]*Institute for High Energy Physics, Protvino 142281*
[20]*INFN—Sezione di Torino, 10125 Torino*
[21]*Institute for Theoretical and Experimental Physics, Moscow 117218*
[22]*J. Stefan Institute, 1000 Ljubljana*
[23]*Kanagawa University, Yokohama 221-8686*
[24]*Kennesaw State University, Kennesaw, Georgia 30144*
[25]*King Abdulaziz City for Science and Technology, Riyadh 11442*
[26]*Korea Institute of Science and Technology Information, Daejeon 305-806*
[27]*Korea University, Seoul 136-713*
[28]*Kyungpook National University, Daegu 702-701*
[29]*École Polytechnique Fédérale de Lausanne (EPFL), Lausanne 1015*
[30]*Faculty of Mathematics and Physics, University of Ljubljana, 1000 Ljubljana*

0031-9007/15/115(14)/142001(7)

[31]Luther College, Decorah, Iowa 52101
[32]University of Maribor, 2000 Maribor
[33]Max-Planck-Institut für Physik, 80805 München
[34]School of Physics, University of Melbourne, Victoria 3010
[35]Middle East Technical University, 06531 Ankara
[36]Moscow Physical Engineering Institute, Moscow 115409
[37]Moscow Institute of Physics and Technology, Moscow Region 141700
[38]Graduate School of Science, Nagoya University, Nagoya 464-8602
[39]Kobayashi-Maskawa Institute, Nagoya University, Nagoya 464-8602
[40]Nara Women's University, Nara 630-8506
[41]National Central University, Chung-li 32054
[42]Department of Physics, National Taiwan University, Taipei 10617
[43]H. Niewodniczanski Institute of Nuclear Physics, Krakow 31-342
[44]Niigata University, Niigata 950-2181
[45]Osaka City University, Osaka 558-8585
[46]Pacific Northwest National Laboratory, Richland, Washington 99352
[47]Peking University, Beijing 100871
[48]University of Pittsburgh, Pittsburgh, Pennsylvania 15260
[49]University of Science and Technology of China, Hefei 230026
[50]Seoul National University, Seoul 151-742
[51]Soongsil University, Seoul 156-743
[52]University of South Carolina, Columbia, South Carolina 29208
[53]Sungkyunkwan University, Suwon 440-746
[54]School of Physics, University of Sydney, New South Wales 2006
[55]Department of Physics, Faculty of Science, University of Tabuk, Tabuk 71451
[56]Tata Institute of Fundamental Research, Mumbai 400005
[57]Excellence Cluster Universe, Technische Universität München, 85748 Garching
[58]Toho University, Funabashi 274-8510
[59]Tohoku University, Sendai 980-8578
[60]Department of Physics, University of Tokyo, Tokyo 113-0033
[61]Tokyo Institute of Technology, Tokyo 152-8550
[62]Tokyo Metropolitan University, Tokyo 192-0397
[63]University of Torino, 10124 Torino
[64]CNP, Virginia Polytechnic Institute and State University, Blacksburg, Virginia 24061
[65]Wayne State University, Detroit, Michigan 48202
[66]Yamagata University, Yamagata 990-8560
[67]Yonsei University, Seoul 120-749

(Received 30 June 2015; published 29 September 2015)

Using a sample of 771.6×10^6 $\Upsilon\Upsilon(4S)$ decays collected by the Belle experiment at the KEKB e^+e^- collider, we observe, for the first time, the transition $\Upsilon(4S) \to \eta h_b(1P)$ with the branching fraction $\mathcal{B}[\Upsilon(4S) \to \eta h_b(1P)] = (2.18 \pm 0.11 \pm 0.18) \times 10^{-3}$ and we measure the $h_b(1P)$ mass $M_{h_b(1P)} = (9899.3 \pm 0.4 \pm 1.0)\ \mathrm{MeV}/c^2$, corresponding to the hyperfine (HF) splitting $\Delta M_{\mathrm{HF}}(1P) = (0.6 \pm 0.4 \pm 1.0)\ \mathrm{MeV}/c^2$. Using the transition $h_b(1P) \to \gamma\eta_b(1S)$, we measure the $\eta_b(1S)$ mass $M_{\eta_b(1S)} = (9400.7 \pm 1.7 \pm 1.6)\ \mathrm{MeV}/c^2$, corresponding to $\Delta M_{\mathrm{HF}}(1S) = (59.6 \pm 1.7 \pm 1.6)\ \mathrm{MeV}/c^2$, the $\eta_b(1S)$ width $\Gamma_{\eta_b(1S)} = (8^{+6}_{-5} \pm 5)\ \mathrm{MeV}/c^2$ and the branching fraction $\mathcal{B}[h_b(1P) \to \gamma\eta_b(1S)] = (56 \pm 8 \pm 4)\%$.

DOI: 10.1103/PhysRevLett.115.142001 PACS numbers: 14.40.Pq, 12.38.Qk, 12.39.Hg, 13.20.Gd

The bottomonium system, comprising bound states of b and $\bar{b}$ quarks, has been studied extensively in the past [1,2]. The recent observations of unexpected hadronic transitions from the $J^{PC} = 1^{--}$ states above the $B\bar{B}$ meson threshold, $\Upsilon(4S)$ and $\Upsilon(5S)$, to lower mass bottomonia have opened new pathways to the elusive spin-singlet states, the $h_b(nP)$ and $\eta_b(nS)$ [3,4], and challenged theoretical descriptions, showing a large violation of the selection rules that apply to transitions below the threshold.

Hadronic transitions between the lowest mass quarkonium levels can be described using the QCD multipole expansion [5–10]. In this approach, the heavy quarks emit two gluons that subsequently transform into light hadrons. The $\pi\pi$ and η transitions between the vector states proceed via emission of $E1E1$ and $E1M2$ gluons, respectively.

Therefore, η transitions are highly suppressed as they require a spin flip of the heavy quark [11,12]. Indeed, the ratio of branching fractions

$$\mathcal{R}^{\eta S}_{\pi\pi S}(n,m) = \frac{\mathcal{B}[\Upsilon(nS) \to \eta\Upsilon(mS)]}{\mathcal{B}[\Upsilon(nS) \to \pi^+\pi^-\Upsilon(mS)]},$$

is measured to be small for low-lying states: $\mathcal{R}^{\eta S}_{\pi\pi S}(2,1) = (1.64 \pm 0.23) \times 10^{-3}$ [13–15] and $\mathcal{R}^{\eta S}_{\pi\pi S}(3,1) < 2.3 \times 10^{-3}$ [14].

Above the $B\bar{B}$ threshold, *BABAR* observed the transition $\Upsilon(4S) \to \eta\Upsilon(1S)$ with the unexpectedly large branching fraction of $(1.96 \pm 0.28) \times 10^{-4}$, corresponding to $\mathcal{R}^{\eta S}_{\pi\pi S}(4,1) = 2.41 \pm 0.42$ [16]. This apparent violation of the heavy quark spin-symmetry was explained by the contribution of B meson loops or, equivalently, by the presence of a four-quark $B\bar{B}$ component inside the $\Upsilon(4S)$ wave function [17,18]. At the $\Upsilon(5S)$ energy, the anomaly is even more striking. The spin-flip processes $\Upsilon(5S) \to \pi\pi h_b(1P,2P)$ are found not to be suppressed with respect to the spin-symmetry preserving reactions $\Upsilon(5S) \to \pi\pi\Upsilon(1S,2S)$ [3], and all the $\pi\pi$ transitions show the presence of new resonant structures [19,20] that cannot be explained as conventional bottomonium states.

Further insight into the mechanism of the hadronic transitions above the threshold can be gained by searching for the $E1M1$ transition $\Upsilon(4S) \to \eta h_b(1P)$, which is predicted to have a branching fraction of the order of 10^{-3} [21].

In this Letter, we report the first observation of the $\Upsilon(4S) \to \eta h_b(1P)$ transition and the measurement of the $h_b(1P)$ and $\eta_b(1S)$ resonance parameters. Following the approach used for the observation of the $h_b(1P,2P)$ production in e^+e^- collisions at the $\Upsilon(5S)$ energy [3]—by studying the inclusive $\pi^+\pi^-$ missing mass in hadronic events—we investigate the missing mass spectrum of η mesons in the $\Upsilon(4S)$ data sample. The missing mass is defined as $M_{\mathrm{miss}}(\eta) = \sqrt{(P_{e^+e^-} - P_\eta)^2}$, where $P_{e^+e^-}$ and P_η are the four-momenta of the colliding e^+e^- pair and the η meson, respectively.

The large sample of reconstructed $h_b(1P)$ events allows us to measure its mass and, via the $h_b(1P) \to \gamma\eta_b(1S)$ transition, the mass and width of the $\eta_b(1S)$. The latter are especially important since there is a 3.2σ discrepancy between the $\eta_b(1S)$ mass measurement by Belle using $h_b(1P,2P) \to \gamma\eta_b(1S)$ transitions [4] and by *BABAR* and CLEO using $\Upsilon(2S,3S) \to \gamma\eta_b(1S)$ [22–24].

This analysis is based on the 711 fb^{-1} sample collected at the center-of-mass energy of $\sqrt{s} = 10.580\ \mathrm{GeV}/c^2$ by the Belle experiment [25,26] at the KEKB asymmetric-energy e^+e^- collider [27–29], corresponding to 771.6×10^6 $\Upsilon(4S)$ decays. Monte Carlo (MC) samples are generated using EvtGen [30]. The detector response is simulated with GEANT3 [31]. Separate MC samples are generated for each run period to account for the changing detector performance and accelerator conditions.

Candidate events are requested to satisfy the standard Belle hadronic selection [32], to have at least three charged tracks pointing towards the primary interaction vertex, a visible energy greater than $0.2\sqrt{s}$, a total energy deposition in the electromagnetic calorimeter (ECL) between $0.1\sqrt{s}$ and $0.8\sqrt{s}$, and a total momentum balanced along the z axis. Continuum $e^+e^- \to q\bar{q}$ events (where $q \in \{u,d,s,c\}$) are suppressed by requiring R_2, the ratio of the second to zeroth Fox-Wolfram moment [33], to be less than 0.3. The η candidates are reconstructed in the dominant $\eta \to \gamma\gamma$ channel. The γ candidates are selected from energy deposits in the ECL that have a shape compatible with an electromagnetic shower, and are not associated with charged tracks. We investigate the absolute photon energy calibration using three calibration samples: $\pi^0 \to \gamma\gamma$, $\eta \to \gamma\gamma$, and $D^{*0} \to D^0\gamma$ [4]. Comparing the peak position and the widths of the three calibration signals in the MC sample and in the data, as a function of the photon energy E, we determine the photon energy correction $\mathcal{F}_{\mathrm{en}}(E) < 0.1\%$ and the resolution correction factor $\mathcal{F}_{\mathrm{res}}(E) \approx (+5 \pm 3)\%$. We recalibrate the ECL response by adding to the energy of the reconstructed clusters, E_{rec}, the quantity $\Delta E = \mathcal{F}_{\mathrm{en}}E_{\mathrm{rec}} + \mathcal{F}_{\mathrm{res}}(E_{\mathrm{rec}} - E_{\mathrm{gen}})$, where E_{gen} is the energy of the photon originating the cluster. An energy threshold, ranging from 50 to 95 MeV, is applied as a function of the polar angle to reject low energy photons arising from the beam-related backgrounds. To reject photons from π^0 decays, $\gamma\gamma$ pairs having invariant mass within 17 MeV$/c^2$ of the nominal π^0 mass [34] are identified as π^0 candidates and the corresponding photons are excluded from the η reconstruction process. The angle θ between the photon direction and that of the $\Upsilon(4S)$ in the η rest frame peaks at $\cos(\theta) \approx 1$ for the remaining combinatorial background. Thus, we require $\cos(\theta) < 0.94$ for the η selection. All the selection criteria are optimized using the MC simulation by maximizing the figure of merit $f = N_{\mathrm{sig}}/\sqrt{N_{\mathrm{sig}} + N_{\mathrm{bkg}}}$, where N_{sig} and N_{bkg} are the signal and background yields in the signal region, respectively. The η peak in the $\gamma\gamma$ invariant mass distribution, after the selection is applied, can be fit by a crystal ball (CB) [35] probability density function (PDF) with a resolution of 13 MeV$/c^2$. Thus, $\gamma\gamma$ pairs with an invariant mass within 26 MeV$/c^2$ of the nominal η mass m_η [34] are selected as a signal sample, while the candidates in the regions $39\ \mathrm{MeV}/c^2 < |M(\gamma\gamma) - m_\eta| < 52\ \mathrm{MeV}/c^2$ are used as control samples. To improve the $M_{\mathrm{miss}}(\eta)$ resolution, a mass-constrained fit is performed on the η candidates in both the signal and control regions. The resulting $M_{\mathrm{miss}}(\eta)$ distribution is shown in the inset of Fig. 1. The $\Upsilon(4S) \to \eta h_b(1P)$ and $\Upsilon(4S) \to \eta\Upsilon(1S)$ peaks in $M_{\mathrm{miss}}(\eta)$ are modeled with CB PDFs, whose Gaussian core resolutions

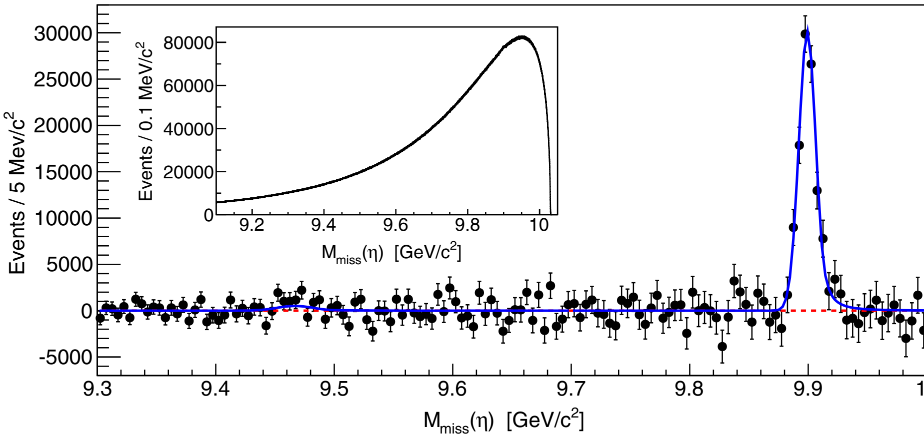

FIG. 1 (color online). $M_{\text{miss}}(\eta)$ distribution after the background subtraction. The solid blue curve shows the fit with the signal PDFs, while the dashed red curve represents the background only hypothesis. The inset shows the $M_{\text{miss}}(\eta)$ distribution before the background subtraction.

are fixed according to the MC simulation. The parameters of the non-Gaussian tails, which account for the effects of the soft initial state radiation (ISR), are calculated assuming the next-to-leading order formula for the ISR emission probability [36] and by modeling the $\Upsilon(4S)$ as a Breit-Wigner resonance with $\Gamma = (20.5 \pm 2.5)\ \text{MeV}/c^2$ [34]. The $M_{\text{miss}}(\eta)$ spectrum is fitted in two separate intervals: (9.30, 9.70) and (9.70, 10.00) GeV/c^2. In the first (second) interval, the combinatorial background is described with a sixth-order (11th) Chebyshev polynomial. The polynomial order is determined maximizing the confidence level of the fit and is validated using sideband samples. Figure 1 shows the background-subtracted $M_{\text{miss}}(\eta)$ distribution, with a bin size 50 times larger than that used for the fit. The confidence levels of the fits are 1% in the lower interval and 19% in the upper one. The transition $\Upsilon(4S) \to \eta h_b(1P)$ is observed with a statistical significance of 11σ, calculated using the profile likelihood method [37], and no signal is observed in the $\gamma\gamma$-mass control regions. The $h_b(1P)$ yield is $N_{h_b(1P)} = 112469 \pm 5537$. From the position of the peak, we measure $M_{h_b(1P)} = (9899.3 \pm 0.4 \pm 1.0)\ \text{MeV}/c^2$ (hereinafter, the first error is statistical and the second is systematic). We calculate the branching fraction of the transition as

$$\mathcal{B}[\Upsilon(4S) \to \eta h_b(1P)] = \frac{N_{h_b(1P)}}{N_{\Upsilon(4S)}\epsilon_{\eta h_b(1P)}\mathcal{B}[\eta \to \gamma\gamma]},$$

where $N_{\Upsilon(4S)} = (771.6 \pm 10.6) \times 10^6$ is the number of $\Upsilon(4S)$, $\epsilon_{\eta h_b(1P)} = (16.96 \pm 1.12)\%$ is the reconstruction efficiency and $\mathcal{B}[\eta \to \gamma\gamma] = (39.41 \pm 0.21)\%$ [34]. We obtain $\mathcal{B}[\Upsilon(4S) \to \eta h_b(1P)] = (2.18 \pm 0.11 \pm 0.18) \times 10^{-3}$, in agreement with theoretical predictions [21]. No evidence of $\Upsilon(4S) \to \eta\Upsilon(1S)$ is present, so we set the 90% confidence level (C.L.) upper limit $\mathcal{B}[\Upsilon(4S) \to \eta\Upsilon(1S)] < 2.7 \times 10^{-4}$, in agreement with the previous experimental result by *BABAR* [16]. All the upper limits presented in this Letter are obtained using the CL_s technique [38,39] and include systematic uncertainties. Using our measurement of $M_{h_b(1P)}$, we calculate the corresponding $1P$ hyperfine (HF) splitting, defined as the difference between the $\chi_{bJ}(1P)$ spin-averaged mass $m^{\text{sa}}_{\chi_{bJ}(1P)}$ and the $h_b(1P)$ mass, and obtain $\Delta M_{\text{HF}}(1P) = (+0.6 \pm 0.4 \pm 1.0)\ \text{MeV}/c^2$; the systematic error includes the uncertainty on the value of $m^{\text{sa}}_{\chi_{bJ}(1P)}$ [34].

As validation of our measurement, we study the $\eta \to \pi^+\pi^-\pi^0$ mode. The π^0 candidate is reconstructed from a $\gamma\gamma$ pair with invariant mass within 17 MeV/c^2 of the nominal π^0 mass [34] while the $\pi^\pm$ candidates tracks are required to be associated with the primary interaction vertex and not identified as kaons by the particle identification algorithm. We observe an excess in the signal region with statistical significance of 3.5σ and measure $\mathcal{B}[\Upsilon(4S) \to \eta h_b(1P)]_{\eta\to\pi^+\pi^-\pi^0} = (2.3 \pm 0.6) \times 10^{-3}$, which is in agreement with the result from the $\gamma\gamma$ mode.

TABLE I. Systematic uncertainties in the determination of $\mathcal{B}[\Upsilon(4S) \to \eta h_b(1P)]$, in units of %, and on $M_{h_b(1P)}$, in units of MeV/c^2.

Source	$\mathcal{B}$	$M_{h_b(1P)}$
Fit range and background PDF order	±2.4	±0.1
Bin width	±2.5	±0.1
ISR modeling	±2.8	±0.7
Peaking backgrounds	±0.5	±0.4
γ energy calibration	±1.2	±0.3
Reconstruction efficiency	±6.6	...
$N_{\Upsilon(4S)}$	±1.4	...
Beam energy	±0.0	±0.4
$\mathcal{B}[\eta \to \gamma\gamma]$	±0.5	...
Total	±8.2	±1.0

The contributions to the systematic uncertainty in our measurements are summarized in Table I. To estimate them, we first vary—simultaneously—the fit ranges within $\pm 100\ \mathrm{MeV}/c^2$ and the order of the background polynomial between 7 (4) and 14 (8) in the upper (lower) interval. The average variation of the fitted parameters when the fitting conditions are so changed is adopted as the fit-range or model systematic uncertainty. Similarly, we vary the bin width between 0.1 and 1 MeV/c^2, and we treat the corresponding average variations as the bin-width systematic error. The ISR modeling contribution is due to the $\Upsilon(4S)$ width uncertainty [34]. The presence of peaking backgrounds is studied using MC samples of inclusive $B\bar{B}$ events and bottomonium transitions. While no peaking background due to B meson decay has been identified, the as-yet-unobserved transitions $\Upsilon(4S) \to \gamma\gamma\Upsilon(1^3D_{1,2}) \to \gamma\gamma\eta\Upsilon(1S)$ can appear as a peak in the $M_{\mathrm{miss}}(\eta)$ spectrum; this contribution is modeled as a CB PDF with a peak at $M_{\mathrm{miss}}(\eta) = 9.877\ \mathrm{GeV}/c^2$ and a resolution of $10.6\ \mathrm{MeV}/c^2$. No significant $\Upsilon(4S) \to \gamma\gamma\Upsilon(1^3D_{1,2}) \to \gamma\gamma\eta\Upsilon(1S)$ signal is observed under these assumptions, and we obtain an upper limit on the product of branching fractions $\mathcal{B}[\Upsilon(4S) \to \gamma\gamma\Upsilon(1^3D_{1,2})] \times \mathcal{B}[\Upsilon(1^3D_{1,2}) \to \eta\Upsilon(1S)] < 0.8 \times 10^{-4}$ (90% C.L.). The uncertainty on the photon energy calibration factors is determined by varying both $\mathcal{F}_{\mathrm{en}}(E)$ and $\mathcal{F}_{\mathrm{res}}(E)$ within their errors. The uncertainty on the reconstruction efficiency includes contributions from several sources. Using 121.4 fb^{-1} collected at the $\Upsilon(5S)$ energy, the $\Upsilon(5S) \to \pi^+\pi^-\Upsilon(2S)$ transition is reconstructed; the comparison of the R_2 distribution obtained from this data sample with the simulation suggests a $\pm 3\%$ uncertainty related to the continuum rejection. A $\pm 1\%$ uncertainty is assigned for the efficiency of the hadronic event selection. The uncertainty on the photon reconstruction efficiency is estimated using $D \to K^\pm\pi^\mp\pi^0$ events to be $\pm 2.8\%$ per photon, corresponding to $\pm 5.6\%$ per η. The number of $\Upsilon(4S)$ mesons is measured with a relative uncertainty of $\pm 1.4\%$ from the number of hadronic events after the subtraction of the continuum contribution using off-resonance data. The absolute value of accelerator beam energies are calibrated by fully reconstructed B mesons. The uncertainty on the B meson mass [34] limits the precision on $M_{h_b(1P)}$ to $\pm 0.4\ \mathrm{MeV}/c^2$, while it has a negligible effect on the branching ratio measurement. Finally, we include an uncertainty in the branching fraction due to the uncertainty in $\mathcal{B}[\eta \to \gamma\gamma]$ [34].

The study of the $\eta_b(1S)$ is performed by reconstructing the transitions $\Upsilon(4S) \to \eta h_b(1P) \to \eta\gamma\eta_b(1S)$. To extract the signal, we measure the number of $\Upsilon(4S) \to \eta h_b(1P)$ events $N_{h_b(1P)}$ as a function of the variable $\Delta M_{\mathrm{miss}} = M_{\mathrm{miss}}(\eta\gamma) - M_{\mathrm{miss}}(\eta)$, where $M_{\mathrm{miss}}(\eta\gamma)$ is the missing mass of the $\eta\gamma$ system. The signal transition will produce a peak in $N_{h_b(1P)}$ at $m_{\eta_b(1S)} - m_{h_b(1P)}$. The radiative photon arising from the $h_b(1P)$ decay is reconstructed with the same criteria used in the $\eta \to \gamma\gamma$ selection, and the $h_b(1P)$ yield in each ΔM_{miss} bin is measured with the fitting procedure described above. To assure the convergence of the $M_{\mathrm{miss}}(\eta)$ fit in each ΔM_{miss} interval, the $h_b(1P)$ mass is fixed to $9899.3\ \mathrm{MeV}/c^2$, the range is reduced to $(9.80, 9.95)\ \mathrm{GeV}/c^2$ and the order of the background PDF polynomial is decreased to seven. The $h_b(1P)$ yield as a function of ΔM_{miss}, shown in Fig. 2, exhibits an excess at $\Delta M_{\mathrm{miss}} = M_{\eta_b(1S)} - M_{h_b(1P)}$ with a statistical significance of 9σ. The $\eta_b(1S)$ peak is described by the convolution of a double-sided CB PDF, whose parameters are fixed according to the MC simulation, and a nonrelativistic Breit-Wigner PDF that accounts for the natural $\eta_b(1S)$ width. The background is described by an exponential. We measure $M_{\eta_b(1S)} - M_{h_b(1P)} = (-498.6 \pm 1.7 \pm 1.2)\ \mathrm{MeV}/c^2$, $\Gamma_{\eta_b(1S)} = (8^{+6}_{-5} \pm 5)\ \mathrm{MeV}/c^2$, and the number of $\Upsilon(4S) \to \eta h_b(1P) \to \eta\gamma\eta_b(1S)$ events $N_{\eta_b(1S)} = 33116 \pm 4741$. The confidence level of the fit is 50%. We calculate the branching fraction of the radiative transition as

$$\mathcal{B}[h_b(1P) \to \gamma\eta_b(1S)] = \frac{N_{\eta_b(1S)}\epsilon_{\eta h_b(1P)}}{N_{h_b(1P)}\epsilon_{\eta\gamma\eta_b(1S)}},$$

where $\epsilon_{\eta h_b(1P)}/\epsilon_{\eta\gamma\eta_b(1S)} = 1.887 \pm 0.053$ is the ratio of the reconstruction efficiencies for $\Upsilon(4S) \to \eta h_b(1P)$ and $\Upsilon(4S) \to \eta h_b(1P) \to \eta\gamma\eta_b(1S)$. We obtain $\mathcal{B}[h_b(1P) \to \gamma\eta_b(1S)] = (56 \pm 8 \pm 4)\%$. To estimate the systematic uncertainties reported in Table II, we adopt the methods discussed earlier. Uncertainties related to the $M_{\mathrm{miss}}(\eta)$ fit are determined by changing the fit range, the bin width, the background-polynomial order, and the fixed values of $M_{h_b(1P)}$ used in the fits. Similarly, the uncertainties arising from the ΔM_{miss} fit are studied by repeating it with different ranges and binning. The calibration uncertainty accounts for

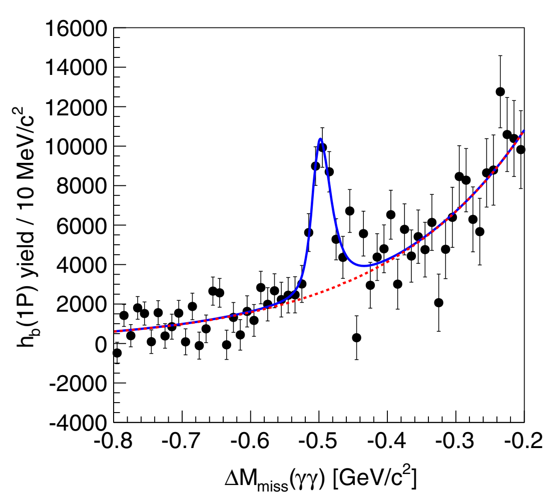

FIG. 2 (color online). ΔM_{miss} distribution. The blue solid curve shows our best fit, while the dashed red curve represents the background component.

TABLE II. Systematic uncertainties in the determination of the $\eta_b(1S)$ mass and width in units of MeV/c^2, and on $\mathcal{B} = \mathcal{B}[h_b(1P) \to \gamma\eta_b(1S)]$ in units of %.

Source	$\Delta M_{\rm miss}$	$\Gamma_{\eta_b(1S)}$	$\mathcal{B}$
$M_{\rm miss}(\eta)$ fit range	± 0.8	± 3.0	± 2.8
$M_{\rm miss}(\eta)$ bin width	± 0.0	± 0.1	± 0.0
$M_{\rm miss}(\eta)$ polynomial order	± 0.1	± 1.9	± 1.6
$M_{h_b(1P)}$	± 0.0	± 0.8	± 1.1
$\Delta M_{\rm miss}$ fit range	± 0.0	± 0.7	± 2.2
$\Delta M_{\rm miss}$ bin width	± 0.8	± 2.8	± 5.2
γ energy calibration	± 0.5	± 0.3	± 1.2
Reconstruction efficiency ratio	$\cdots$	$\cdots$	± 2.8
Total	± 1.2	± 4.7	± 7.2

the errors on the photon energy calibration factors. The uncertainty due to the ratio of the reconstruction efficiencies arises entirely from the single-photon reconstruction efficiency. The $\eta_b(1S)$ annihilates into two gluons, while the $h_b(1P)$ annihilates predominantly into three gluons, but the MC simulation indicates no significant difference in the R_2 distribution. Therefore, the continuum suppression cut does not contribute to the uncertainty arising from the reconstruction efficiency ratio. We calculate the $\eta_b(1S)$ mass as $M_{\eta_b(1S)} = M_{h_b(1P)} + \Delta M_{\rm miss} = (9400.7 \pm 1.7 \pm 1.6)\,{\rm MeV}/c^2$. Assuming $m_{\Upsilon(1S)} = (9460.30 \pm 0.26)\,{\rm MeV}/c^2$ [34], we calculate $\Delta M_{\rm HF}(1S) = (59.6 \pm 1.7 \pm 1.6)$ MeV/c^2.

A summary of the results presented in this Letter is shown in Table III. We report the first observation of a single-meson transition from spin-triplet to spin-singlet bottomonium states, $\Upsilon(4S) \to \eta h_b(1P)$. This process is found to be the strongest known transition from the $\Upsilon(4S)$ meson to lower bottomonium states. A new measurement of the $h_b(1P)$ mass is presented. The corresponding $1P$ hyperfine splitting is compatible with zero, which can be interpreted as evidence of the absence of sizable long range spin-spin interactions. Exploiting the radiative transition $h_b(1P) \to \gamma\eta_b(1S)$, we present a new measurement of the mass difference between the $h_b(1P)$ and the $\eta_b(1S)$ and, assuming our measurement of $M_{h_b(1P)}$, we calculate $M_{\eta_b(1S)}$. Our result is in agreement with the value obtained with the $\Upsilon(5S) \to \pi^+\pi^- h_b(1P) \to \pi^+\pi^-\gamma\eta_b(1S)$ process [4] but exhibits a discrepancy with the measurements based on the $M1$ transitions $\Upsilon(2S, 3S) \to \gamma\eta_b(1P)$ [22–24]. From the theoretical point of view, our result is in agreement with the predictions of many potential models and lattice calculations [40], including the recent lattice result in Ref. [41]. Our measurement of $\mathcal{B}[h_b(1P) \to \gamma\eta_b(1S)]$ agrees with the theoretical predictions [42,43]. All the direct measurements presented in this Letter are independent of the previous results reported by Belle [3], which were obtained by reconstructing different transitions and using a different data sample. Furthermore, all the results, except for $\Delta M_{\rm HF}(1S)$ and $\Delta M_{\rm HF}(1P)$, are obtained using the new analysis described in this Letter and are, therefore, uncorrelated with the existing world averages.

TABLE III. Summary of the results of the searches for $\Upsilon(4S) \to \eta h_b(1P)$ and $h_b(1P) \to \gamma\eta_b(1S)$.

Observable	Value
$\mathcal{B}[\Upsilon(4S) \to \eta h_b(1P)]$	$(2.18 \pm 0.11 \pm 0.18) \times 10^{-3}$
$\mathcal{B}[h_b(1P) \to \gamma\eta_b(1S)]$	$(56 \pm 8 \pm 4)\%$
$M_{h_b(1P)}$	$(9899.3 \pm 0.4 \pm 1.0)$ MeV/c^2
$M_{\eta_b(1S)} - M_{h_b(1P)}$	$(-498.6 \pm 1.7 \pm 1.2)$ MeV/c^2
$\Gamma_{\eta_b(1S)}$	$(8^{+6}_{-5} \pm 5)$ MeV/c^2
$M_{\eta_b(1S)}$	$(9400.7 \pm 1.7 \pm 1.6)$ MeV/c^2
$\Delta M_{\rm HF}(1S)$	$(+59.6 \pm 1.7 \pm 1.6)$ MeV/c^2
$\Delta M_{\rm HF}(1P)$	$(+0.6 \pm 0.4 \pm 1.0)$ MeV/c^2

We thank the KEKB group for excellent operation of the accelerator; the KEK cryogenics group for efficient solenoid operations; and the KEK computer group, the NII, and PNNL/EMSL for valuable computing and SINET4 network support. We acknowledge support from MEXT, JSPS, and Nagoya's TLPRC (Japan); ARC and DIISR (Australia); FWF (Austria); NSFC (China); MSMT (Czechia); CZF, DFG, and VS (Germany); DST (India); INFN (Italy); MOE, MSIP, NRF, GSDC of KISTI, and BK21Plus (Korea); MNiSW and NCN (Poland); MES (particularly under Contract No. 14.A12.31.0006), RFAAE and RFBR under Grant No. 14-02-01220 (Russia); ARRS (Slovenia); IKERBASQUE and UPV/EHU (Spain); SNSF (Switzerland); NSC and MOE (Taiwan); and DOE and NSF (USA).

[1] N. Brambilla, S. Eidelman, B. K. Heltsley, R. Vogt, G. T. Bodwin, E. Eichten, A. D. Frawley, A. B. Meyer *et al.*, Eur. Phys. J. C **71**, 1534 (2011).
[2] N. Brambilla *et al.*, Eur. Phys. J. C **74**, 2981 (2014).
[3] I. Adachi *et al.* (Belle Collaboration), Phys. Rev. Lett. **108**, 032001 (2012).
[4] R. Mizuk *et al.* (Belle Collaboration), Phys. Rev. Lett. **109**, 232002 (2012).
[5] K. Gottfried, Phys. Rev. Lett. **40**, 598 (1978).
[6] G. Bhanot, W. Fischler, and S. Rudaz, Nucl. Phys. **B155**, 208 (1979).
[7] M. E. Peskin, Nucl. Phys. **B156**, 365 (1979).
[8] G. Bhanot and M. E. Peskin, Nucl. Phys. **B156**, 391 (1979).
[9] M. B. Voloshin, Nucl. Phys. **B154**, 365 (1979).
[10] M. B. Voloshin and V. I. Zakharov, Phys. Rev. Lett. **45**, 688 (1980).
[11] Y.-P. Kuang, Front. Phys. China **1**, 19 (2006).
[12] M. B. Voloshin, Prog. Part. Nucl. Phys. **61**, 455 (2008).
[13] Q. He *et al.* (CLEO Collaboration), Phys. Rev. Lett. **101**, 192001 (2008).
[14] J. P. Lees *et al.* (*BABAR* Collaboration), Phys. Rev. D **84**, 092003 (2011).
[15] U. Tamponi *et al.* (Belle Collaboration), Phys. Rev. D **87**, 011104 (2013).

[16] B. Aubert *et al.* (*BABAR* Collaboration), Phys. Rev. D **78**, 112002 (2008).
[17] C. Meng and K. T. Chao, Phys. Rev. D **78**, 074001 (2008).
[18] M. B. Voloshin, Mod. Phys. Lett. A **26**, 773 (2011).
[19] A. Bondar *et al.* (Belle Collaboration), Phys. Rev. Lett. **108**, 122001 (2012).
[20] P. Krokovny *et al.* (Belle Collaboration), Phys. Rev. D **88**, 052016 (2013).
[21] F.-K. Guo, C. Hanhart, and Ulf.-G. Meissner, Phys. Rev. Lett. **105**, 162001 (2010).
[22] B. Aubert *et al.* (*BABAR* Collaboration), Phys. Rev. Lett. **101**, 071801 (2008); **102**, 029901(E) (2009).
[23] B. Aubert *et al.* (*BABAR* Collaboration), Phys. Rev. Lett. **103**, 161801 (2009).
[24] G. Bonvicini *et al.* (CLEO Collaboration), Phys. Rev. D **81**, 031104 (2010).
[25] A. Abashian *et al.*, Nucl. Instrum. Methods Phys. Res., Sect. A **479**, 117 (2002).
[26] J. Brodzicka *et al.* (Belle Collaboration), Prog. Theor. Exp. Phys. (**2012**) 04D001.
[27] S. Kurokawa and E. Kikutani, Nucl. Instrum. Methods Phys. Res., Sect. A **499**, 1 (2003), and other papers included in this volume.
[28] T. Abe *et al.*, Prog. Theor. Exp. Phys. (**2013**) 03A001.
[29] T. Abe *et al.*, Prog. Theor. Exp. Phys. (**2013**) 03A006, and the other papers included in Prog. Theor. Exp. Phys., Volume 2013 Issue 3 (March 2013).
[30] D. J. Lange, Nucl. Instrum. Methods Phys. Res., Sect. A **462**, 152 (2001).
[31] R. Brun *et al.*, GEANT3.21, CERN Report No. DD/EE/84-1, 1984.
[32] K. Abe *et al.* (Belle Collaboration), Phys. Rev. D **64**, 072001 (2001).
[33] G. C. Fox and S. Wolfram, Phys. Rev. Lett. **41**, 1581 (1978).
[34] K. A. Olive *et al.* (Particle Data Group), Chin. Phys. C, **38**, 090001 (2014).
[35] J. Gaiser *et al.*, Phys. Rev. D **34**, 711 (1986).
[36] M. Benayoun, S. I. Eidelman, V. N. Ivanchenko, and Z. K. Silagadze, Mod. Phys. Lett. A **14**, 2605 (1999).
[37] G. Cowan, K. Cranmer, E. Gross, and O. Vitells, Eur. Phys. J. C **71**, 1554 (2011).
[38] T. Junk, Nucl. Instrum. Methods Phys. Res., Sect. A **434**, 435 (1999).
[39] A. Read, J. Phys. G **28**, 2693 (2002).
[40] T. J. Burns, Phys. Rev. D **87**, 034022 (2013).
[41] R. J. Dowdall, C. T. H. Davies, T. Hammant, and R. R. Horgan (HPQCD Collaboration), Phys. Rev. D **89**, 031502 (R) (2014).
[42] S. Godfrey and J. L. Rosner, Phys. Rev. D **66**, 014012 (2002).
[43] D.-Y. Chen, X. Liu, and T. Matsuki, Phys. Rev. D **87**, 094010 (2013).